Superoxide dismutase mimetic properties exhibited by vacancy engineered ceria nanoparticles†

Cassandra Korsvik,[a] Swanand Patil,[b] Sudipta Seal[b] and William T. Self*[a]

Received (in Berkeley, CA, USA) 18th October 2006, Accepted 3rd January 2007
First published as an Advance Article on the web 23rd January 2007
DOI: 10.1039/b615134e

In this report ceria nanoparticles are shown to act as catalysts that mimic superoxide dismutase (SOD) with the catalytic rate constant exceeding that determined for the enzyme SOD.

Cerium is a rare earth element of the lanthanide series. The oxide form (CeO_2) has routinely been used in polishing glass, but current research is focused on use of cerium oxide nanoparticles in catalytic converters for automobile exhaust systems, oxygen sensors, an electrolyte for solid oxide fuel cells or as an ultraviolet absorbent.[1–4] While most of the rare earths exist in trivalent state (+3), cerium also occurs in tetravalent (+4) state and may flip-flop between the two in a redox reaction.[5–8] It is established that cerium oxides make excellent oxygen buffers, because of this redox capacity.[9] As a result of alterations in the cerium oxidation state, cerium oxide forms oxygen vacancies or defects in the lattice structure by loss of oxygen and/or its electrons.[6,7] The valence and defect structure of cerium oxide is dynamic and may change spontaneously or in response to physical parameters such as temperature, presence of other ions, and partial pressure of oxygen.[5,6,10] Studies have shown that with a decrease in particle size, cerium oxide nanoparticles show a formation of more oxygen vacancies.[11] The increased surface area to volume in nanoparticles enables CeO_2 to regenerate its activity and thereby act catalytically. In the case of transition metal oxides, a thorough analysis of vacancies has lead to the understanding of the fundamental nature of the catalytic reactivity.[12–15] This knowledge has been lacking in the rare earth oxides. In addition, there has been no reported literature on the molecular mechanism of any catalytic activity of these nanoparticles in biological systems.

Cerium oxide nanoparticles have a unique electron structure that is similar to chemical spin traps such as nitrosone compounds, and mixed valence state ceria nanoparticles have been recently shown to apparently act as biological antioxidants.[16] It has been proposed that this antioxidant activity is mediated at oxygen vacancies at the surface. If so, then one cerium oxide nanoparticle may offer many sites for catalysis, whereas pharmacological agents or enzymes offer only one active site per molecule. In addition, the electron defects in ceria nanoparticles may not be destroyed after their initial reaction with reactive oxygen species and thus these nanoparticles may be potent catalysts in a living cell. Although there is growing evidence that ceria nanoparticles impart protection to living cells,[16] the molecular mechanism of the antioxidant properties of cerium oxide nanoparticles has yet to be elucidated.

Previous studies have suggested, based on observations of the impact of ceria nanoparticles on cultured cells, that ceria nanoparticles can act as radical scavengers and redox cycling antioxidants.[16–18] In this report we evaluated the ability of mixed valence state ceria nanoparticles (with higher levels of cerium in the +3 state) to react with superoxide *in vitro*. Since it has been proposed that surface oxygen vacancies can mediate catalysis on ceria nanostructures, and that higher ratio of Ce^{3+}/Ce^{4+} in nanoparticles preparation correlates with higher oxygen and electron vacancy,[11,19] we tested two preparations of ceria nanoparticles in this study for their ability to react with superoxide. First, we analyzed two ceria nanoparticle preparations for their size, X-ray diffraction pattern and surface chemistry. HRTEM analysis shows that preparation A (Fig. 1A, ESI†) consists of polycrystalline particles with 3–5 nm crystals. Sample B (Fig. 1B, ESI†) consists of

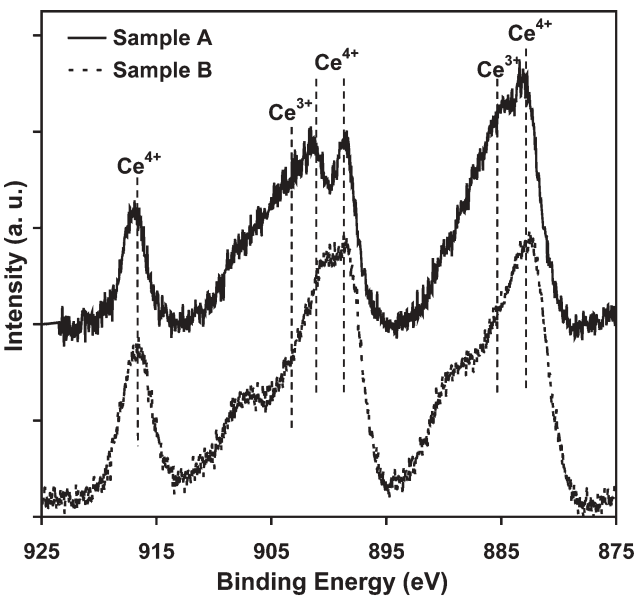

Fig. 1 Ce 3d high resolution XPS analysis reveals higher Ce^{3+} levels in sample A compared to sample B. The peaks between 875–895 eV correspond to Ce $3d_{5/2}$, between 895–910 eV correspond to Ce $3d_{3/2}$ and peak at 916 eV is a characteristic satellite peak indicating the presence of +4 states. The peaks at 880.2, 885.0, 899.5 and 903.5 eV are indicative of +3 peaks as opposed to those at 882.1, 888.1, 898.0, 900.9, 906.4 and 916.40 eV indicating the presence of +4 states.[11] Note, the population density of +3 states in Sample A is higher than in Sample B.

[a]*Department of Molecular Biology and Microbiology, Burnett College of Biomedical Sciences, University of Central Florida, Orlando, Florida 32816, USA. E-mail: wself@mail.ucf.edu; Fax: +1 (407) 823-0956; Tel: +1(407) 823-4262*
[b]*Advanced Materials Processing and Analysis Center, Nanoscience and Technology Center (NSTC), University of Central Florida, Orlando, Florida 32816, USA*

† Electronic supplementary information (ESI) available: Detailed methods and two supplemental figures. See DOI: 10.1039/b615134e

hard, agglomerated, relatively large (5–8 nm) particles. The lattice fringes of the particles showed the allowed planes (111) and (200) in the particles. Theoretical calculations have shown that the (111) surface is the most stable plane in cerium oxide.[5]

Next we used X-ray diffraction (XRD) analysis (Fig. 2, ESI†) to confirm that both preparations of ceria nanoparticles contain a fluorite crystal lattice. Peak broadening in sample A confirmed the smaller particle size compared to sample B, which is consistent with the HRTEM analysis. The measured BET (Brunauer Emmett Teller) surface areas were also consistent with the HRTEM and XRD measurements. The specific surface areas of the samples A and B were found to be 140 and 115 $m^2\ g^{-1}$, respectively. The Ce (3d) XPS spectra shown in Fig. 1 demonstrates the presence of a mixed valence state (Ce^{3+} and Ce^{4+}) for both preparations. These results are similar to our previously published results of cerium oxide nanoparticles.[11,20] Higher intensity peaks corresponding to Ce^{3+} were observed in sample A, indicating a higher Ce^{3+}/Ce^{4+} ratio in this sample. The Ce (3d) XPS spectra were deconvoluted as described previously[11] and the concentration of Ce^{3+} was calculated using the equation:

$$[Ce^{3+}] = \frac{A_{vo} + A_{v'} + A_{u0} + A_{u'}}{A_{vo} + A_{v'} + A_{u0} + A_{u'} + A_{v} + A_{v} + A_{v'} + A_{u} + A_{u} + A_{u'}}$$

where, A_i is the integrated area of peak i.

The Ce^{3+} concentration in sample A was found to be 40 atom% while that in sample B was 22 atom%. These results are in line with our earlier studies of size dependent changes in valence state of cerium oxide nanoparticles which indicated increase in Ce^{3+} with decrease in particle size.[11] These two nanoparticles preparations allowed us to compare ceria preparation with varying surface chemistry for their potential interaction with superoxide.

We then tested whether nanoceria would affect the level of hydrogen peroxide produced in the presence of superoxide (generated from hypoxanthine/xanthine oxidase). We observed a significant increase in hydrogen peroxide levels produced in the presence of ceria nanoparticles using a coupled horseradish peroxidase assay (data not shown). This increase was observed in both preparations of nanoparticles, but the apparent increase was more dramatic with preparation A. Since we had observed increases in hydrogen peroxide production in the presence of ceria nanoparticles and superoxide, we then tested the activity of ceria nanoparticles in a classic SOD activity assay—competition with cytochrome C for reduction by superoxide. Indeed, nanoparticle preparation A efficiently competed with ferricytochrome C for reduction by superoxide (Fig. 2B) in a concentration dependent manner. Preparation B also displayed some SOD mimetic activity as well, but this was far less efficient, as indicated by the poor competition with ferricytochrome C (Fig. 2C). Addition of EDTA at concentrations up to 5 mM did not alter the activity, confirming that adventitious iron or other metal was not catalyzing the activity (data not shown). The concentration of SOD in the reaction shown in Figure 6A (1 unit addition) is 120 nM. Since this is significantly higher than the particle concentration, this suggests that each nanoceria molecule is a more efficient catalyst that SOD.

Using a comparative method for SOD kinetic analysis previously described[21] and the known rate constant for reduction of ferricytochrome C by superoxide at pH 7.2 ($1.1 \times 10^5\ M^{-1}\ s^{-1}$), we determined the catalytic rate constant for nanoceria preparation A (with respect to the average nanoparticle) to be

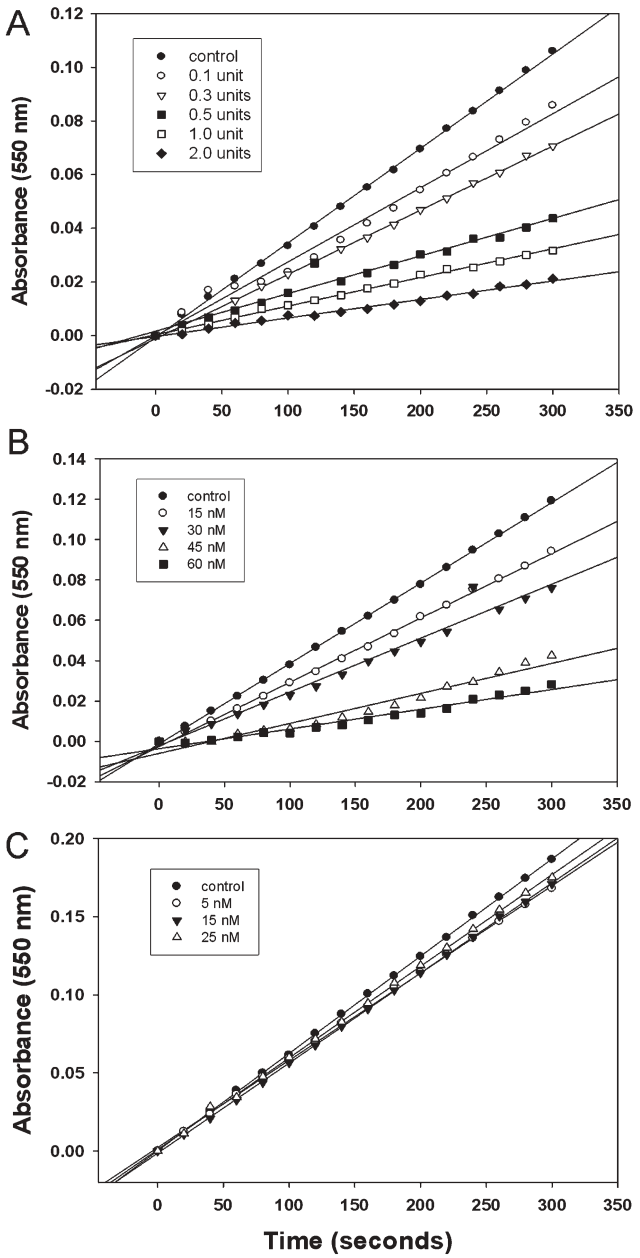

Fig. 2 SOD mimetic activity of ceria nanoparticles assayed using ferricytochrome C. Ferricytochrome C reduction was followed spectrophotometrically by measuring the increase in absorbance at 550 nm. Two thousand units of catalase were added to the reaction to efficiently remove hydrogen peroxide and avoid side reactions with ferricytochrome C or ceria nanoparticles. Ceria nanoparticle concentrations were determined by calculating the average diameter of particles (using TEM, above Fig 1) in the preparation, and conversion to particle concentration based on total ceria in solution. A. CuZnSOD was added to a reaction where reduction of ferricytochrome C was occurring at a rate of 0.025 per min ($A_{550\ nm}$). One unit of CuZnSOD corresponds to an enzyme concentration of 120 nM. B. ceria nanoparticle preparation A was added at 15, 30, 45 and 60 nM concentrations. C. Ceria nanoparticles preparation B was added at 5, 15 and 25 nM concentrations. A representative experiment is shown from at least six replicates (of each concentration of cerium nanoparticles) where the resulting change in the slope of the line (compared to control) varied by less than 20%.

$3.6 \times 10^9\ M^{-1}\ s^{-1}$. The most recent kinetic analysis of CuZn SOD calculated a rate constant for SOD between 1.3 and $2.8 \times 10^9\ M^{-1}\ s^{-1}$, depending on the reaction conditions. Thus a single ceria nanoparticle is more efficient as an SOD catalyst than the authentic enzyme itself.

Nanoparticles have larger surface energy due to a large surface to volume ratio, and this property makes them more reactive compared to their bulk counterparts. Cerium oxide nanoparticles form oxygen vacancies by giving out oxygen from their crystal lattice. Previous studies have shown that size of ceria nanoparticles negatively correlates with the ratio of Ce^{3+}/Ce^{4+}.[11] Experiment evidence presented here clearly demonstrate that ceria nanoparticles with higher Ce^{3+}/Ce^{4+} ratio catalyze SOD mimetic activity, yet the molecular mechanism behind this catalysis is still unknown. The SOD mimetic activity exhibited by the vacancy engineered ceria nanoparticles is likely to be the mechanism of action for data previously presented that showed protection of cells against ROS or demonstrated a lifespan extension with treatment with ceria nanoparticles.[16–18]

Although the 'active site' of the ceria nanoparticle has yet to be firmly established, one can speculate on the reaction mechanism based on that known for SOD. Similar to Fe and Mn-SOD it is possible that the dismutation of superoxide by ceria nanoparticles is catalyzed as follows:

$$O_2^{\bullet -} + Ce^{4+} \rightarrow O_2 + Ce^{3+}$$

$$O_2^{\bullet -} + Ce^{3+} + 2H^+ \rightarrow H_2O_2 + Ce^{4+}$$

Catalysis could occur at the same cerium atom (as in the case with the metal-dependent SOD) or independently at different oxygen vacancy sites. Future studies to determine the molar ratio of products, and to elucidate the site of catalysis by the ceria nanoparticles will shed light on this interesting questions raised by the data presented in this report.

This work was supported by NSF grant (BES0541516) to S.S. and W.T.S.

Notes and references

1 G. A. Deluga, J. R. Salge, L. D. Schmidt and X. E. Verykios, *Science*, 2004, **303**, 993–997.
2 K. Otsuka, *Chem. Lett.*, 1993, **9**, 1517–1520.
3 A. Trovarelli, *Catalysis by ceria and related materials*, Imperial College Press, London, 2002.
4 S. Park, J. M. Vohs and R. J. Gorte, *Nature*, 2000, **404**, 265–267.
5 J. C. Conesa, *Surf. Sci.*, 1995, **339**, 337–352.
6 G. S. Herman, *Surf. Sci.*, 1999, **437**, 207–214.
7 T. Suzuki, I. Kosacki, H. U. Anderson and P. Colomban, *J. Am. Ceram. Soc.*, 2001, **84**, 2007–2014.
8 F. Esch, S. Fabris, L. Zhou, T. Montini, C. Africh, P. Fornasiero, G. Comelli and R. Rosei, *Science*, 2005, **309**, 752–755.
9 P. L. Land, *J. Phys. Chem. Solids*, 1973, **34**, 1839–1845.
10 E. Mamontov, T. Egami, R. Brezny, M. Koranne and S. Tyagi, *J. Phys. Chem. B*, 2000, **104**, 11110–11116.
11 S. Deshpande, S. Patil, S. Kuchibhatla and S. Seal, *Appl. Phys. Lett.*, 2005, **87**, 133113.
12 C. T. Campbell, *Science*, 2003, **299**, 357.
13 R. Schaub, E. Wahlstrom, A. Ronnau, E. Lagsgaard, I. Stensgaard and F. Besenbacher, *Science*, 2003, **299**, 377–379.
14 E. Wahlstrom, E. K. Vestergaard, R. Schaub, A. Ronnau, M. Vestergaard, E. Laegsgaard, I. Stensgaard and F. Besenbacher, *Science*, 2004, **303**, 511–513.
15 M. D. Rasmussen, L. M. Molina and B. Hammer, *J. Chem. Phys.*, 2004, **120**, 988–997.
16 R. W. Tarnuzzer, J. Colon, S. Patil and S. Seal, *Nano Lett.*, 2005, **5**, 2573–2577.
17 B. A. Rzigalinski, *Technol. Cancer Res. Treat.*, 2005, **4**, 651–660.
18 B. A. Rzigalinski, D. Bailey, L. Chow, S. C. Kuiry, S. Patil, S. Merchant and S. Seal, *FASEB J.*, 2003, **17**, A606–A606.
19 J. Y. Ying and A. Tschope, *Chem. Eng. J. Biochem. Eng. J.*, 1996, **64**, 225–237.
20 S. Patil, S. C. Kuiry and S. Seal, *Proc. R. Soc. London, Ser. A*, 2004, **460**, 3569–3587.
21 H. J. Forman and I. Fridovich, *Arch. Biochem. Biophys.*, 1973, **158**, 396–400.
22 T. L. Barr and S. Seal, *J. Vac. Sci. Technol., A*, 1995, **13**, 1239–1246.
23 I. Fridovich, *J. Biol. Chem.*, 1970, **245**, 4053–4057.

